High resolution inclinometer based on vertical pendulum and fiber Bragg grating Fabry–Perot cavity

Peng Cui (崔 鹏)[1,2], Wentao Zhang (张文涛)[2,3,*], and Ying Song (宋 颖)[1]

[1]*School of Traffic and Transportation, Shijiazhuang Tiedao University, Shijiazhuang 050043, China*
[2]*State Key Laboratory of Transducer Technology, Institute of Semiconductors, Chinese Academy of Sciences, Beijing 100083, China*
[3]*College of Materials Science and Opto-Electronic Technology, University of Chinese Academy of Sciences, Beijing 100049, China*
**Corresponding author: zhangwt@semi.ac.cn*

Received July 30, 2018; accepted September 29, 2018; posted online October 31, 2018

In this paper, an inclinometer based on a vertical pendulum and a fiber Bragg grating Fabry–Perot cavity (FBG-FP) is proposed. A low-damping rotation structure is used to reduce the mechanical frictions of the pendulum system and induce a wavelength shift of FBG-FPs. We find that the sensitivity can be maximized by optimizing the parameters of the inclinometer. Using a high-resolution demodulation system, a sensitivity of 179.9 pm/(°), and a resolution better than 0.02″ can be achieved. Experiments also show that the proposed inclinometer has good linearity and repeatability.

OCIS codes: 060.3735, 060.2370.
doi: 10.3788/COL201816.110603.

Inclinometers are widely used in many fields, such as civil infrastructure health monitoring, safety monitoring in the petrochemical industry and electric power engineering, and earthquake monitoring[1,2]. Various types of optical fiber-based tilt sensors have been developed owing to their advantages compared with conventional electric sensors, such as high sensitivity, feasibility in multiplexing, and immunity to electromagnetic interference[3]. One type of fiber optic tilt sensor is based on fiber tapers[4,5]. Some intensity demodulated optical fiber inclinometers based on a tapered-tilted fiber Bragg grating (TFBG) have been developed, and the experimental results show a good relationship between the bending angle and the intensity of the core mode[6]. Fiber taper is easily fabricated but its mechanical strength is reduced. Another type of fiber optic tilt sensor is based on a fiber Bragg grating (FBG)[7,8]. Commercially available FBGs and interrogators result in low cost and good consistency. But the sensitivity and resolution need to be improved, especially in the fields such as railway subgrade settlement or earthquake monitoring.

First, the resolution of an FBG tilt sensor is limited by the demodulation of the Bragg wavelength shift of FBGs[9,10]. The resolution of the wavelength shift of an FBG is limited by its reflection spectrum bandwidth[11]. Compared with a common FBG, the reflection spectrum bandwidth of a fiber Bragg grating Fabry–Perot cavity (FBG-FP) is much narrower, which means a higher wavelength resolution can be achieved. Second, the sensitivity and consistency of the FBG tilt sensor are determined by the performance of the pendulum-based structure, which induces the errors associated with mechanical frictions and limits the resolution[12,13].

In this paper, we propose an inclinometer based on a vertical-pendulum using a blade-edge-type rotation structure as the transducer and FBG-FPs as the sensing element. The proposed pendulum-based fiber inclinometer is shown in Fig. 1. A blade edge and a V-shaped groove are the rotation part of the pendulum system. The pendulum, the blade, and the beam are fixed together. The blade is embedded in a slot under the beam and hung on the V-shaped groove on the supporting structure, which makes the rotation plane orthogonal to the blade edge. Because the blade edge is very sharp and its contact area with the V-shaped groove can be considered as a line, the rotational friction of the pendulum can be significantly reduced. Two FBG-FPs are stretched between the beam and base. The pre-stress is applied by hanging the identical counterweight block (25 g) on two optical fibers and can be calculated through the following equation: $\sigma = mg / A$, where σ is the pre-stress in the fiber, mg is

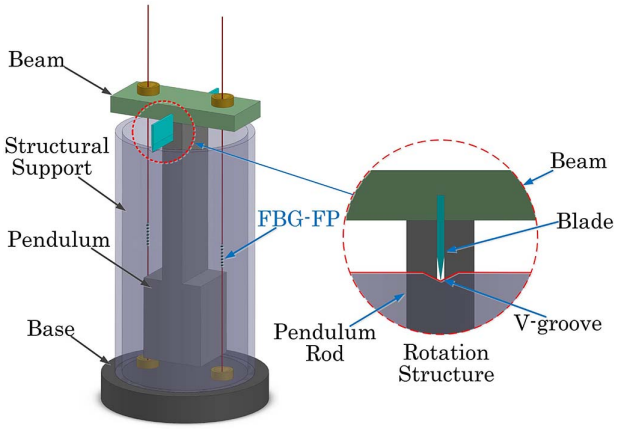

Fig. 1. Structure of the pendulum-based inclinometer and the blade-edge-type rotation structure.

the weight of the counterweight block ($25g$), A is the cross-sectional area of the fiber, and the pre-stress σ is 19.92 MPa. In our experiment, the maximum inclination angle is about 2° and the inclination-induced stress in the fiber is 16.69 MPa according to Eqs. (2) and (3). The prior strain should be larger than the maximum of the strain variation. The pre-stress in the two FBG-FPs is equal and balances the pendulum at its initial position. Owing to the merits of this design, low internal damping of the pendulum is realized, which can improve the sensitivity and repeatability of the inclinometer.

When the inclinometer is tilted to an angle θ, the pendulum will rotate around the edge of the blade due to the gravity. The rotation will induce the strain in the FBG-FP and change the output wavelength of the FBG-FP. The tension in the FBG-FP will make the pendulum deviate from the plumb line. However, the gravity will make the pendulum have a "draw-back" rotation in a small angle θ_1, as shown in Fig. 2.

The tilt angle θ of the inclinometer can be divided into two parts: the actual rotated angle of pendulum θ_1 and the angle deviated from the plumb line θ_2. For small angle variations, $\sin\theta \approx \theta$. According to the theory of the mechanics of materials, θ_1 can be expressed as

$$\theta_1 = \frac{2l_f \cdot \varepsilon}{l}, \tag{1}$$

where ε is the strain of the fiber, l_f is the length of the fiber between the two fixing points, and l is the distance between two parallel optical fibers. Referring to the theory of the mechanics of materials and force analysis in the equilibrium condition, θ_2 is given by

$$T = E\varepsilon A, \tag{2}$$

$$T \cdot \frac{l}{2} = mg \cdot \theta_2 \cdot L, \tag{3}$$

where T is the tension force in the fiber, E is the Young's modulus of the fiber, A is the cross-sectional area of the fiber, m is the mass of the pendulum, and L is the length of the vertical pendulum. Combining Eqs. (1)–(3), we have

$$\theta = \theta_1 + \theta_2 = \frac{2l_f \cdot \varepsilon}{l} + \frac{E\varepsilon A \cdot l}{2mgL} = \varepsilon\left(\frac{2l_f}{l} + \frac{EA \cdot l}{2mgL}\right). \tag{4}$$

The peak wavelength of FBG-FP1 and FBG-FP2 is λ_1 and λ_2, respectively, and $\lambda_1 \approx \lambda_2$. The spectra of the two FBG-FPs are shown in Fig. 3. FBG-FP1 and FBG-FP2 are both "push-pull" structures and the relation can be given as

$$\frac{\Delta\lambda_1 - \Delta\lambda_2}{\lambda_1} = 2 \cdot (1 - P_e)\varepsilon, \tag{5}$$

where P_e is the photoelastic coefficient of the optical fiber. Thus, the sensitivity of the inclinometer can be written as

$$S = \frac{\Delta\lambda_1 - \Delta\lambda_2}{\theta} = 2 \cdot (1 - P_e)\frac{\lambda_1}{\frac{2l_f}{l} + \frac{EAl}{2mgL}}. \tag{6}$$

From the equations above, we know that the inclination sensitivity can be doubled by using two FBG-FPs. In addition, the temperature fluctuations can be discriminated by subtracting the temperature-induced wavelength shift of the FBG-FP1 from the shift of the FBG-FP2, so the proposed sensor configuration completely eliminates the cross-sensitivity that arises from the thermo-optic effects in FBG-FPs. The two FBG-FPs can be used as references for each other to avoid the influence of the temperature fluctuations and translational motion. The wavelength separation $\Delta\lambda_1 - \Delta\lambda_2$ is in linear relationship with the tilt angle for small inclinations. The sensitivity can be improved by increasing the length L or the mass m, as well as reducing the length l_f, and can be maximized by optimizing the parameter l. A curvilinear graph is plotted

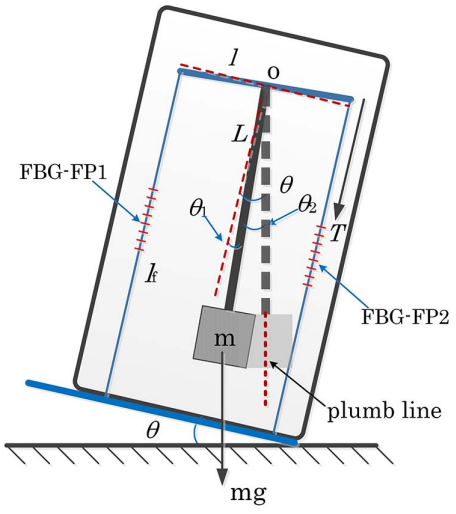

Fig. 2. Schematic diagram of the pendulum-based inclinometer.

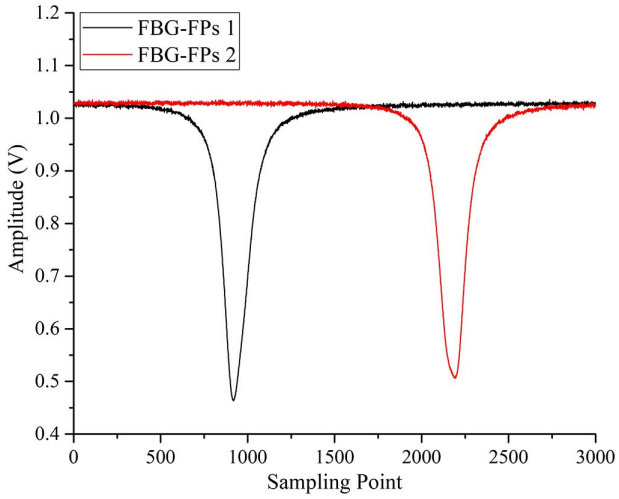

Fig. 3. Spectra of the two FBG-FPs.

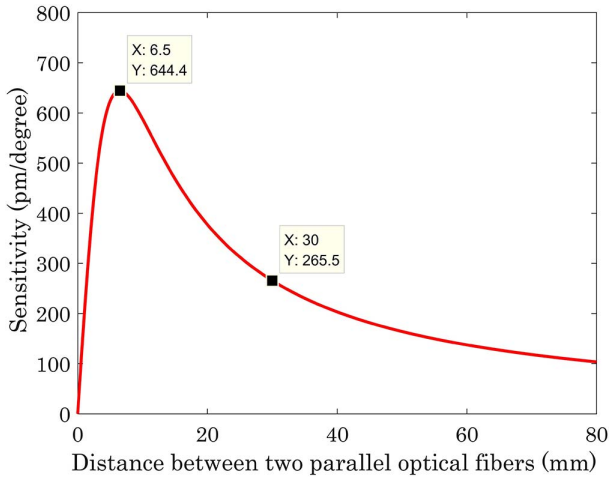

Fig. 4. Sensitivity versus the distance l between two parallel optical fibers.

according to the relationship between the sensitivity and the distance l in Eq. (6), as shown in Fig. 4.

Figure 4 shows that the sensitivity can be maximized when the distance value is 6.5 mm. But it is difficult to realize because of the fabrication technique and the dimension of the components. Therefore, a balance should be found between the distance l and the restrictions above to acquire a higher sensitivity. In our configuration, the minimum distance l is 30 mm. The 3 dB optical reflectivity bandwidth w is about 0.55 nm. The parameters of the configuration are shown in Table 1. According to Eq. (6), the theoretical inclination sensitivity is calculated to be 265.5 pm/(°).

The experimental setup is shown in Fig. 5. The demodulation system is established to demodulate the wavelength shift of the FBG-FPs. The beam from the tunable fiber laser (NKT, linewidth 100 Hz) is split into a pair of FBG-FPs. We employ the polarization controller (PC) to eliminate the effect of polarization instability, and the reflection spectra of the two FBG-FPs are obtained

Table 1. Parameters Used in the Configuration

Parameters	Values
L	45 mm
l	30 mm
l_f	105 mm
m	0.20 kg
g	9.8 m/s^2
E	72 GPa
A	1.23×10^{-8} m^2
P_e	0.22
λ	1537 nm
w	0.55 nm

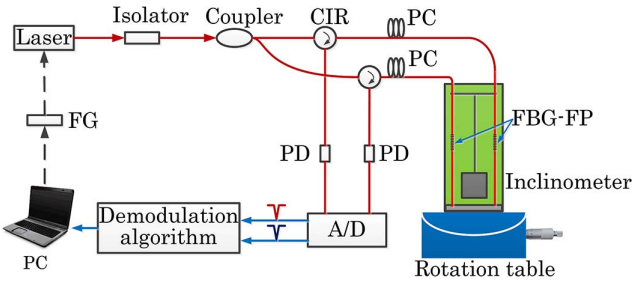

Fig. 5. Experimental setup of the inclinometer.

by photodiode and processed by the cross-correlation method, and the strain of the two FBG-FPs can be demodulated. Owing to the merit of the narrow reflection spectrum bandwidth of the FBG-FP, a very high demodulation resolution of 1×10^{-3} pm can be achieved[14].

The inclinometer, with a cylinder stainless steel shell that can isolate the environmental disturbance, is installed at an inclination calibrated platform. When the inclinometer is tilted, the reflection spectra of FBG-FP1 and FBG-FP2 shift in the opposite direction and wavelength separations of the two FBG-FPs are measured by the demodulator. The tilt angle increases by a step of 370″ in a small range from 0° to 2° and then backward to 0°. This process is considered as one cycle and repeated for three times.

The measured wavelength separations $\Delta\lambda_1 - \Delta\lambda_2$ of the two FBG-FPs among the three cycles are plotted against the tilt angle, as shown in Fig. 6. The experiment results demonstrate a good linearity. The measured tilt angle sensitivity is 179.9 pm/(°). Thus, the resolution of the inclinometer is up to 5.56×10^{-6}° (equal to 0.02″) when the demodulator's resolution is 1×10^{-3} pm. Theoretically, this resolution is approximately 1260 times higher than that of other work measured with FBG[12] or 46,800 times higher than that measured with long-period fiber grating[15]. The measured sensitivity is on the same order of magnitude

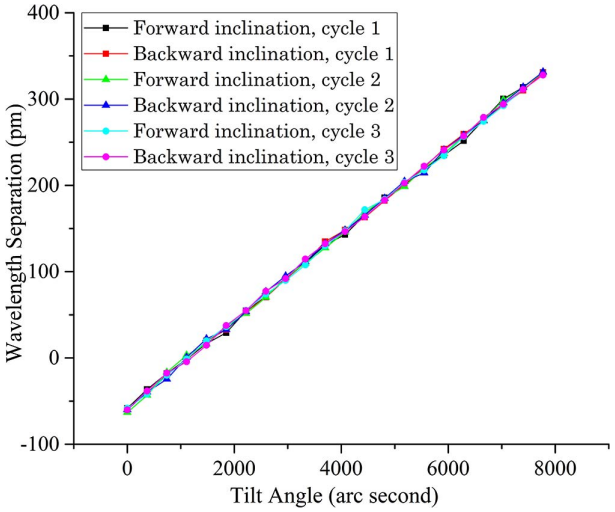

Fig. 6. Relationship between the wavelength separation and tilt angle.

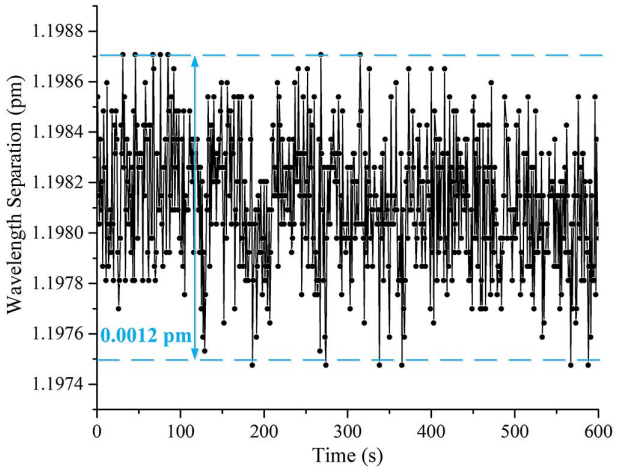

Fig. 7. Wavelength separation during the temperature fluctuation over 10 min.

as the theoretically calculated value, and the discrepancy between them is due to the dimension error in manufacturing the configuration components. Furthermore, the weight of the beam and other connecting parts above the rotation axis is not taken into account when calculating the length of the vertical pendulum, which makes the measured value smaller than the theoretical value. Repeatability of 2.0% and hysteresis less than 1.1% are demonstrated. Compared to the traditional pendulum-based inclinometer, the sensor response is characterized by a definite improvement in reversibility and repeatability over the tilt measuring range of 0° to 2° (limited by the range of now available inclination platforms), which gives the advantage of the low-damping rotation structure.

The fabricated sensor is also put into a temperature test chamber to test the performance of temperature compensation. The wavelength separations $\Delta\lambda_1 - \Delta\lambda_2$ of the two FBG-FPs are measured within the temperature range from 20°C to 70°C, and the result indicates that there is no obvious correlation between the wavelength separations and temperature variations. The data covering 10 min is shown in Fig. 7. The maximum fluctuation of the wavelength shifts of the two FBG-FPs is less than 0.0012 pm. In practical applications, such as earthquake monitoring, the temperature fluctuation of the cavern in which the inclinometer is installed is less than 0.002°C (according to the standards of the China Earthquake Administration), and the total error caused by the temperature variation is about $7.78 \times 10^{-6\circ}$ (equal to $0.028''$), which implies that the temperature cross talk of the inclinometer can be greatly reduced.

However, in this design, there are some shortcomings to be improved upon. For example, the blade edge of the rotation structure is hung on the V-shaped groove and the movement of the pendulum is not restrained along the direction of the rotation axis, which may affect the shock resistance of the sensor. What is more, a lock-pendulum device can be designed to fix the position of the mass to avoid damaging the fibers during sensor's transportation and installation process. All these problems need to be solved in our future work.

In summary, a pendulum-based inclinometer using FBG-FPs as the sensing element and a simple rotation structure with low internal damping has been proposed and demonstrated. Theoretical analysis shows that the sensitivity is enhanced by optimizing the dimension parameters of the inclinometer. Owing to the merits of the specially-designed rotation structure, the inherent friction of the pendulum system can be reduced. The experiment results show that the sensor has good linearity and low temperature response. A tilt angle sensitivity of 179.9 pm/(°) and a high resolution of $5.56 \times 10^{-6\circ}$ have been achieved. Furthermore, the repeatability and stability are significantly improved compared with traditional pendulum-type tilt sensors, which is reflected in a good repeatability of 2.0% and low hysteresis less than 1.1%. The results show that the proposed inclinometer is promising in applications such as earthquake monitoring.

This work was supported by the National Key R&D Program of China (No. 2017YFB0405503), the Youth Innovation Promotion Association of CAS (No. 2016106), the Project of OFCMT (No. SKLD1703), and the Key Project of Hebei Educational Committee (No. BJ2016048).

References

1. H. Y. Chang, Y. C. Chang, and W. F. Liu, Sensors **17**, 2922 (2017).
2. R. Aneesh, M. Maharana, P. Munendhar, H. Y. Tam, and S. K. Khijwania, Appl. Opt. **50**, E172 (2011).
3. R. Yang, H. Bao, S. Zhang, K. Ni, Y. Zheng, and X. Dong, IEEE Sens. J. **15**, 6381 (2015).
4. C.-L. Lee, W.-C. Shih, J.-M. Hsu, and J.-S. Horng, Opt. Express **22**, 24646 (2014).
5. T. Osuch, K. Markowski, A. Manujło, and K. Jędrzejewski, Sens. Actuators A **252**, 76 (2016).
6. C. Guo, D. Chen, C. Shen, Y. Lu, and H. Liu, Opt. Fiber Technol. **24**, 30 (2015).
7. B. J. Peng, Y. Zhao, Y. Zhao, and H. Yang, IEEE Sens. J. **6**, 63 (2006).
8. P. Munendhar, R. Aneesh, and S. K. Khijwania, Appl. Opt. **53**, 3574 (2014).
9. H.-J. Chen, L. Wang, and W. F. Liu, Appl. Opt. **47**, 556 (2008).
10. H. Bao, X. Dong, L. Y. Shao, C. L. Zhao, C. C. Chan, and P. Shum, IEEE Photon. Technol. Lett. **22**, 863 (2010).
11. Z. Liu and H.-Y. Tam, Chin. Opt. Lett. **14**, 120007 (2016).
12. B. O. Guan, H. Y. Tam, and S. Y. Liu, IEEE Photon. Technol. Lett. **16**, 224 (2004).
13. X. Dong, C. Zhan, K. Hu, S. Ping, and C. C. Chan, IEEE Photon. Technol. Lett. **17**, 2394 (2005).
14. W. Huang, W. Zhang, T. Zhen, and F. Zhang, IEEE Photon. Technol. Lett. **26**, 1597 (2014).
15. Y. Wang, C. L. Zhao, L. Hu, X. Dong, Y. Jin, C. Shen, and S. Jin, Rev. Sci. Instrum. **82**, 093106 (2011).